

AD-A141 574

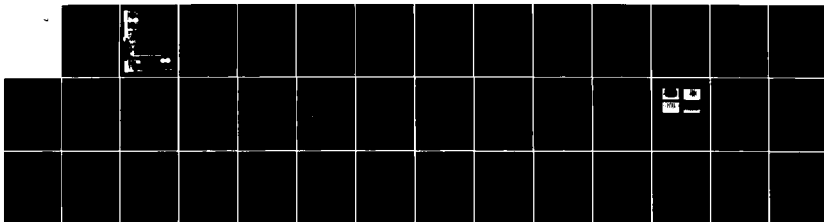
MOLECULAR BEAM EPITAXY OF HOCDE(U) GEORGIA INST OF
TECH ATLANTA ENGINEERING EXPERIMENT STATION
C J SUMMERS ET AL. 30 MAR 84 ARO-17036.3-EL
DAAQ29-80-K-0012

1/1

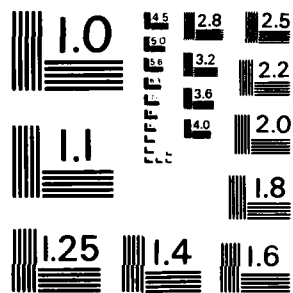
UNCLASSIFIED

F/G 20/2

NL



END
DATE
FILMED
7 84
DTL



MICROCOPY RESOLUTION TEST CHART
NATIONAL BUREAU OF STANDARDS-1963-A

FINAL REPORT

AD-A141 574

MOLECULAR BEAM EPITAXY OF HgCdTe

J. Summers, E. L. Meeks, and N.W. Cox

Prepared for

Army Research Office
Research Triangle Park
North Carolina 27709

Contract No. DAAG29-80-K-0012

GEORGIA INSTITUTE OF TECHNOLOGY

A Unit of the University System of Georgia
Engineering Experiment Station
Atlanta, Georgia 30332

DTIC
ELECTE

MAY 25 1984

A

This document has been approved
for public release and sale; its
distribution is unlimited.

84 05 25 052

MOLECULAR BEAM EPITAXY OF HgCdTe

FINAL REPORT

C. J. Summers, E. L. Meeks, and N. W. Cox

Contract No. DAAG29-80-K-0012

Prepared for:

**Army Research Office
Research Triangle Park
North Carolina 27709**

**Engineering Experiment Station
Georgia Institute of Technology
Atlanta, Georgia 30332**

March 1984

UNCLASSIFIED

SECURITY CLASSIFICATION OF THIS PAGE (When Data Entered)

REPORT DOCUMENTATION PAGE		READ INSTRUCTIONS BEFORE COMPLETING FORM
1. REPORT NUMBER DAAG29-80-K-0012 ARO 17036.3- 4 AD-A242574	2. GOVT ACCESSION NO.	3. RECIPIENT'S CATALOG NUMBER
4. TITLE (and Subtitle) Molecular Beam Epitaxy of HgCdTe	5. TYPE OF REPORT & PERIOD COVERED FINAL REPORT 1980 - Dec. 1983	
7. AUTHOR(s) C. J. Summers, E. L. Meeks and N. W. Cox	6. PERFORMING ORG. REPORT NUMBER	
9. PERFORMING ORGANIZATION NAME AND ADDRESS Engineering Experiment Station Georgia Institute of Technology Atlanta, Georgia 30332	8. CONTRACT OR GRANT NUMBER(s) DAAG-29-80-K-0012	
11. CONTROLLING OFFICE NAME AND ADDRESS U. S. Army Research Office Post Office Box 12211 Research Triangle Park, NC 27709	10. PROGRAM ELEMENT, PROJECT, TASK AREA & WORK UNIT NUMBERS	
14. MONITORING AGENCY NAME & ADDRESS (if different from Controlling Office)	12. REPORT DATE 30 March 1984	
	13. NUMBER OF PAGES 35	
	15. SECURITY CLASS. (of this report) Unclassified	
	15a. DECLASSIFICATION/DOWNGRADING SCHEDULE	
16. DISTRIBUTION STATEMENT (of this Report) Approved for public release; distribution unlimited.		
17. DISTRIBUTION STATEMENT (of the abstract entered in Block 20, if different from Report) NA		
18. SUPPLEMENTARY NOTES The view, opinions, and/or findings contained in this report are those of the author(s) and should not be construed as an official Department of the Army position, policy, or decision, unless so designated by other documentation.		
19. KEY WORDS (Continue on reverse side if necessary and identify by block number) Molecular beam growth Mercury Cadmium Telluride HgCdTe		
20. ABSTRACT (Continue on reverse side if necessary and identify by block number) The design of a molecular beam epitaxial growth system for HgCdTe alloys is described and has been used to grow CdTe and Hg _{1-x} Cd _x Te layers. Investigations of the properties of these layers by reflection electron diffraction, u.v. reflectivity and X-ray diffraction measurements show that at present the quality of CdTe substrates and/or surface preparation procedures cause an initial degradation of the quality of the layer, but that these defects can be grown out. For CdTe layers thicker than 5 microns, good quality		

DD FORM 1 JAN 73 1473

EDITION OF 1 NOV 65 IS OBSOLETE


UNCLASSIFIED

SECURITY CLASSIFICATION OF THIS PAGE (When Data Entered)

✓ surfaces are obtained. Epitaxial deposited CdTe has been shown to be remarkably adaptable and (111) orientated CdTe layers have been grown on (100) orientated GaAs and InP substrates. Mercury cadmium telluride layers with x-values between 0.9 and 0.17 were grown on these CdTe buffer layers and demonstrated good crystal quality with spectral response characteristics extending out to 10 μm at 300K.

TABLE OF CONTENTS

1.	Introduction	1
2.	Theory of MBE Growth of HgCdTe	3
3.	MBE Apparatus and Growth Procedure	7
4.	Material Analysis and Properties	16
5.	Conclusions	29
6.	Technical Presentations and Publications	31
7.	Technical Personnel	33
8.	References	34



Accession For	
NTIS GRA&I	<input checked="" type="checkbox"/>
DTIC TAB	<input type="checkbox"/>
Unannounced	<input type="checkbox"/>
Justification	
By _____	
Distribution/	
Availability Codes	
Dist	Avail and/or Special
A-1	

1. INTRODUCTION

The development of large focal plane arrays is urgently required for thermal imaging systems because of their potential to improve system performance (sensitivity, range or resolution) by several order of magnitude.¹ These array designs must be based on a photovoltaic detector technology in order to minimize array contacts, achieve high packing densities, low power consumption, and signal integration.¹ In addition, the material properties required for these devices are very severe; i.e. low n- and p-type carrier concentrations, long carrier lifetimes and very homogeneous properties over large areas.² Recent results with liquid phase epitaxy have achieved most of these conditions and high-performance HgCdTe photodiodes have been reported.³ However, the processing technology of this material system (p-n junction formation and surface passivation) still presents difficult problems because of stoichiometric doping effects and the non-congruent evaporation of HgCdTe surfaces.⁴

Studies of photodiode structures show that the performance of both 3-5 and particularly 8-14 micron devices is critically dependent on material, interface and surface properties, and can be optimized by the growth of homopolar and heterojunction structures with specific doping and compositional profiles.³ The ability of molecular beam epitaxy to grow similar structures in III-V compounds thus makes it an attractive growth process to consider for the HgCdTe system.⁵

This program was therefore initiated to investigate the feasibility of molecular beam epitaxy growth techniques to grow HgCdTe alloys. The program involved three phases:

- 1) The design of a flexible and versatile MBE system to investigate the growth mechanisms and procedures for growing high vapor pressure and volatile materials such as HgCdTe.
- 2) The use of this apparatus to ascertain the feasibility of growing HgCdTe by MBE.
- 3) The optimization of any procedures developed in (2) to grow low x-valued epitaxial HgCdTe layers.

The apparatus, results, and technical accomplishments of this program are described in the following sections.

2. THEORY OF MBE GROWTH OF HgCdTe

The MBE growth of HgCdTe is significantly different from most materials because of the rapid dissociation of HgCdTe when heated above 90°C⁸ and the high vapor pressure of Hg.⁷ Both of these properties must be considered in establishing the conditions required to grow HgCdTe alloys. Experiments on low x-values HgCdTe alloys show that they evaporate non-congruently with Hg being the predominate evaporated species between 0 - 250°C.⁶ Above 200°C Te₂ begins to evaporate and its equilibrium vapor pressure increases rapidly with increasing temperature to give near congruent evaporation in these alloys above 320°C. The evaporation of Cd is found to be significant only above 450°C.

Thus, provided epitaxial growth can be established below 250°C, where the difference between the vapor pressures of Hg and Te₂ is large (> 100), it is only necessary to consider one volatile component; Hg. The growth considerations for HgCdTe are sketched in Fig. 1, where F_{Hg}^S is the flux of the Hg lost from the surface of the HgCdTe layer, F_{Hg} , F_{Cd} and F_{Te} are the elemental beam fluxes from the growth furnaces and k_{Hg} , k_{Cd} and k_{Te} are the respective sticking coefficients for these elements on the substrate surface. To obtain stoichiometric material, the following conditions must be satisfied at the growth interface

$$(k_{Hg} F_{Hg} - F_{Hg}^S) + k_{Cd} F_{Cd} = \frac{k_{Te} F_{Te_2}}{2} \quad (1)$$

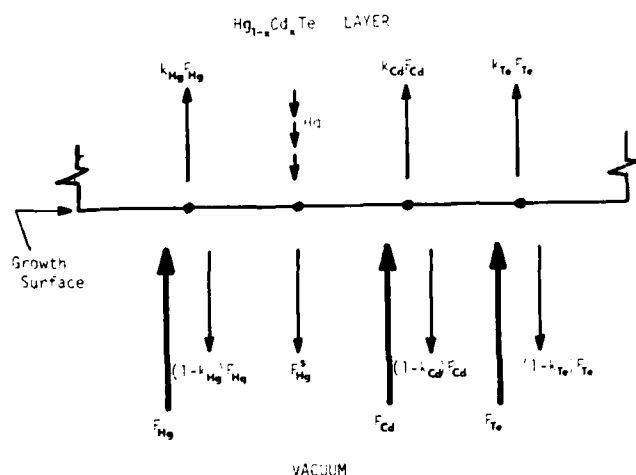


Figure 1. Schematic of growth conditions for $\text{Hg}_{1-x}\text{Cd}_x\text{Te}$ by MBE.

where the factor 2 accounts for the fact that tellurium evaporates as a dimer. For this situation the growth rate, R , is given by

$$R = \frac{2k_{\text{Te}_2} F_{\text{Te}_2}}{N} \text{ cm/S} \quad (2)$$

where N is the number of atoms cm^{-3} in the HgCdTe alloy. The alloy composition, x , is determined by the relative incorporation rates of Hg and Cd into the crystal, i.e.

$$x = \frac{k_{\text{Cd}} F_{\text{Cd}}}{(k_{\text{Hg}} F_{\text{Hg}} - F_{\text{Hg}}^S) + k_{\text{Cd}} F_{\text{Cd}}} \quad (3)$$

Substituting from Eq. 1, this equation becomes

$$x = \frac{2 k_{Cd} F_{Cd}}{k_{Te} F_{Te_2}} \quad (4)$$

Thus provided equation 1 is satisfied, equations 2 and 3 show that the growth rate is determined principally by the Te_2 flux and the alloy composition by the Cd to Te_2 flux ratio. From Eq. 3 the Hg flux required to grow a given alloy composition for a given substrate temperature and growth rate can be calculated provided the sticking coefficients are known. Rearranging Eq. 3 we obtain

$$F_{Hg} = \frac{1}{k_{Hg}} (x F_{Hg}^S + (1 - x) k_{Cd} F_{Cd}) \quad (5)$$

The sticking coefficients of the different components are determined by the thermal energy of the substrate surface and by chemical attachment kinetics. Experiments performed on glass substrates confirmed that no measurable amount of Cd or Hg was deposited when evaporated singly even for substrate temperatures as low as 26°C. Also, experiments performed with Te_2 on glass indicate the sticking coefficient of Te_2 is very close to 1.0 for substrate temperatures as high as 250°C. Thus, for the HgCdTe system, the sticking coefficient of Te_2 is primarily thermally determined and the sticking coefficients of Hg and Cd are

determined by their reaction kinetics with Te_2 . The chemical bond between Cd and Te_2 is much stronger than the bond between Hg and Te_2 , and in the presence of Te_2 , the sticking coefficient of Cd has been determined to be 1.0.⁸ When fluxes of all three elements are incident on the substrate surface, the Cd + Te_2 bond will take precedence; and when there is insufficient Cd to combine with all the Te_2 flux, the difference is made up with Hg. The above argument shows that the growth rate of the $1-x\text{Cd}_x\text{Te}$ alloys is determined primarily by the Te_2 flux and secondarily by the Cd flux plus the amount of the Hg flux necessary to equal the Te_2 flux. It also shows that the x value is determined by the Cd/ Te_2 flux ratio.

3. MBE APPARATUS AND GROWTH PROCEDURE

From the previous discussion it is apparent that the growth of $\text{Hg}_{1-x}\text{Cd}_x\text{Te}$ alloys by molecular beam epitaxy requires special considerations. These considerations concern not only the decomposition of the $\text{Hg}_{1-x}\text{Cd}_x\text{Te}$ layer at low growth temperatures and the low sticking coefficient of Hg, but also the practicality of handling the high Hg vapor pressure.

Because the decomposition rate of $\text{Hg}_{1-x}\text{Cd}_x\text{Te}$ alloys decreases rapidly with decreasing temperature, the first consideration can be alleviated to some extent by growing at low substrate temperatures. However, there is a lower limit placed on the substrate temperature which is determined by the need to grow single crystal material. Essentially, the substrate temperature must be high enough for the absorbed molecules (Hg, Cd and Te_2) to have sufficient energy to migrate along the growth surface so that they solidify in the lowest energy configuration; i.e. form a single crystal. A lower substrate temperature is also expected to increase the Hg sticking coefficient.

The low sticking coefficient⁹ and high vapor pressure of Hg also place special demands on both the design and operation of the MBE system. Firstly, because of the low sticking coefficient, most of the Hg flux is not absorbed on the substrate. Thus, a very high ($>10^{17}\text{cm}^{-2}\text{s}^{-1}$) and continuous Hg-flux density is required to grow low x-valued $\text{Hg}_{1-x}\text{Cd}_x\text{Te}$ layers that are sufficiently thick (> 10 microns) for infrared detector

applications. This makes it essential to use elemental Hg for the Hg-source because a binary compound such as HgTe, will be quickly depleted. Secondly, the high vapor pressure of Hg at room temperature makes it impossible to use as a conventional MBE source material. Either the Hg must be kept at very low temperatures during most of the system operation, or it must be introduced into the high vacuum chamber during the growth cycle. Because the first approach makes the Hg source very susceptible to contamination and would require repeated openings of the system to replenish the Hg charge, the second option was initiated in this work. Lastly, the high Hg vapor pressure makes it essential to have extensive cryoshielding throughout the system and an effective pumping system to limit and quickly remove the excess Hg-vapor during growth and the post-growth bake-out procedure.

From the previous estimate of the critical control parameters required to grow $\text{Hg}_{1-x}\text{Cd}_x\text{Te}$ alloys, it is apparent that because Cd and Te_2 are expected to have near unity sticking coefficients, most of the incident Cd and Te_2 molecular beams will be deposited on the substrate. Thus, the magnitude of the Te_2 flux will determine the anion-to-cation ratio and, therefore, the growth rate. The large difference between the sticking coefficients of Hg and Cd, will result in the Cd always being preferentially absorbed. Thus, provided the Hg is in excess, the Cd flux will determine the composition of the alloy. To first order, the control of the growth process is therefore dependent

on the flux control of the Te₂ and Cd ovens and the stability of the substrate temperature. Ideally, it is desired that upon condensation on to the substrate, all three components should be in precise balance to form a crystalline, homogeneous layer that is in exact stoichiometric balance.

The apparatus designed to investigate the MBE growth requirements for HgCdTe is shown in Figure 2. The system consists of three principal components: a growth chamber, a sample load-lock, and a pumping system. All are constructed from stainless steel and sealed with copper gaskets. The main component of the growth chamber is the furnace module which is cooled to liquid nitrogen temperatures and can hold up to six furnaces. To minimize cross-contamination between the ovens, the growth furnace module is mounted horizontally and the cryoshielding encloses as much as possible of the ovens. The furnace shutters are also cooled through their mountings on the cryo-shielding and are actuated externally by rotatable feed-throughs. The sample growth area is also enclosed by a liquid nitrogen cooled shield and is fitted with a ionization gauge adjacent to the sample for flux rate measurements.

Because the substrate temperatures required for the growth of HgCdTe are expected to be below 300°C and must be well regulated and uniform, a heated air flow systems was used. This system has a temperature stability of <0.1°C and allows the substrate temperature to be abruptly changed by altering the air mix, or if necessary, to be cooled below room temperature. As

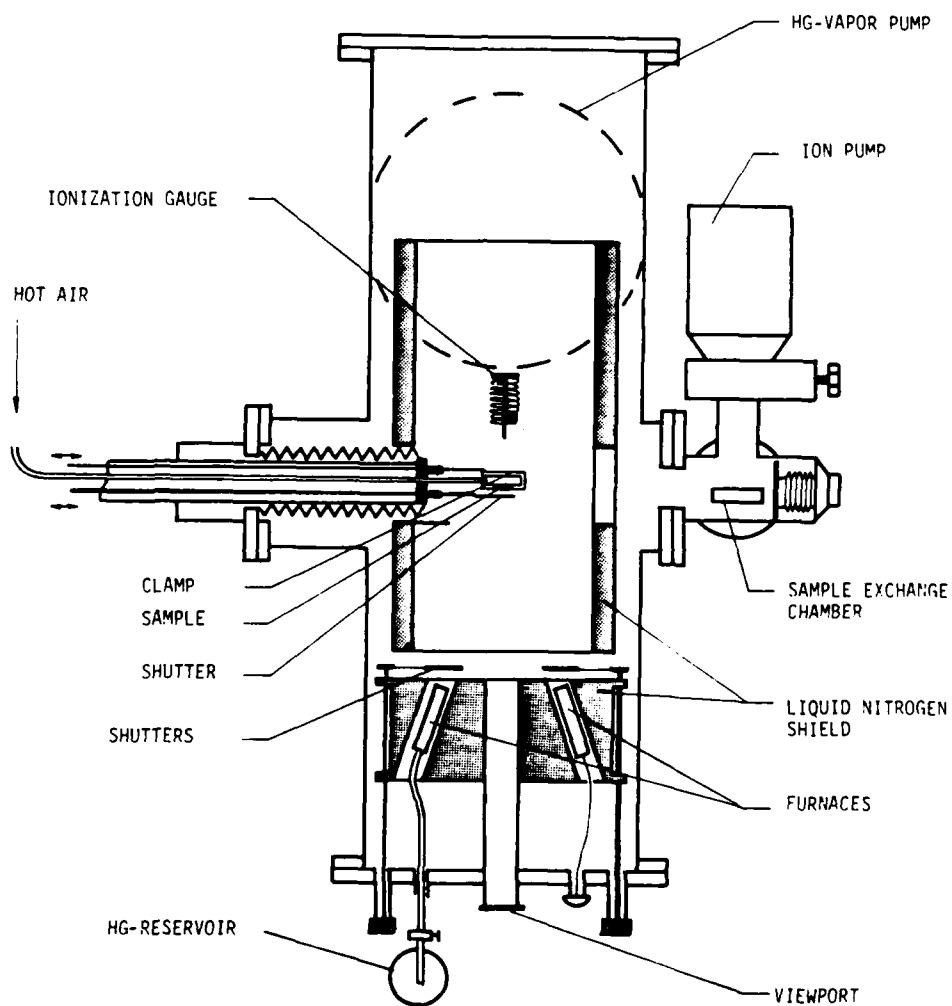


Figure 2. Schematic of MBE apparatus used to grow CdTe and $\text{Hg}_{1-x}\text{Cd}_x\text{Te}$ layers.

shown, the air flow system is mounted externally and connected to the substrate holder through a metal bellows. The sample holder is also fitted with a shutter to allow selective shielding of the substrate during growth.

The vacuum system consists of a sorption pump and an ion pump for the sample load-lock module, and a sorption pump and Hg vapor diffusion pump fitted with two liquid nitrogen cold traps for the growth chamber. These systems typically produce a vacuum in the 10^{-7} and 10^{-9} torr range, respectively, which were sufficient for the initial investigations of the crystalline properties of CdTe and HgCdTe.

The solid state furnaces are of conventional design and are lined with high purity graphite. Their temperatures are controlled and stabilized to a precision of 0.1° by using highly stabilized d.c. power supplies and precision temperature controllers. To permit high-vacuum bake-out and to provide sufficient furnace operational time at the high flux rates required to grow thick HgCdTe layers, the Hg furnace ensemble is separated into two components; an oven to provide flux control and a large reservoir which is mounted externally to the growth chamber. The Hg furnace has a stainless steel lining and is fitted with a small probe to monitor the Hg level. The principal feature of the reservoir is a stainless steel bellows which is attached to a micrometer so that the reservoir volume can be reduced to feed precise quantities of Hg into the oven section.

Because of the high Hg vapor pressure and contamination levels, the design of an efficient (material conserving) Hg-

furnace was essential for growing HgCdTe alloys of the quality and thickness required for infrared detector applications. To reduce the Hg contamination level, it is necessary to reduce the distribution of the flux emitted by the oven and also to condense the Hg reflected from the sample on cryoshields. Initially, the flux from the Hg oven was apertured by the use of liquid nitrogen cryoshields. However, the Hg frozen on the shields reduced the aperture size such that for low x-valued (Hg rich) alloys it became difficult to grow uniform layers thicker than 3 μ m. A reflux two-temperature oven was therefore designed (as shown in Fig. 3) and has to some extent overcome this problem. As shown in the figure, the magnitude of the Hg-flux is established by the temperature of the base of the oven, and the flux is restricted to a cone directed toward the sample by a series of baffles. These are well removed from the Hg melt and with the walls of the top section of the oven are maintained at a temperature that is greater than the freezing point of Hg, but significantly less than the temperature of the base of the oven. For the present system, the Hg temperature is 90°C and the temperature of the top part of the oven is 0°C. This is sufficient to condense Hg onto the surface and to lower its temperature such that the vapor pressure of the condensed Hg is several orders of magnitude less than the main beam. The condensed Hg flows back to the melt along a channel cut in the base of the oven. To prevent Hg-liquid from dripping across the apertures, the inner surfaces are highly polished and angle lips surround each side of the apertures. The

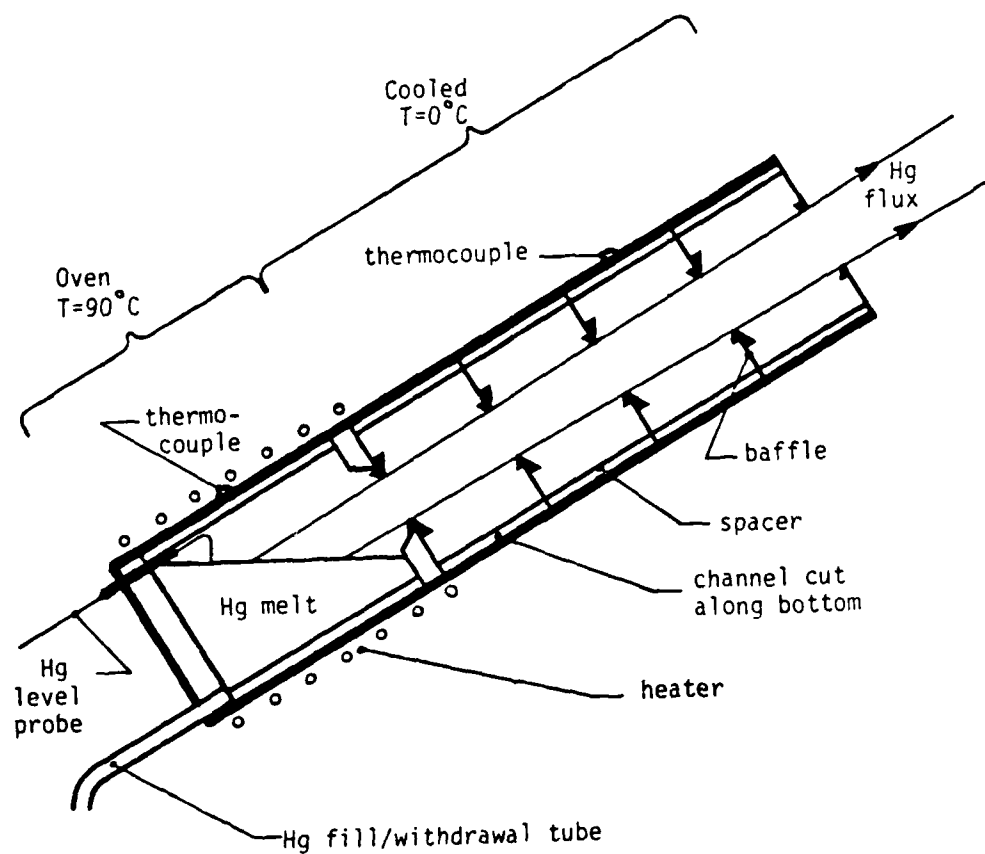


Figure 3. Two-temperature Hg-oven design.

lip facing the flux is made as small as possible to minimize its surface area in the path of the Hg beam.

The system is operated by first loading a sample into a cassette in the load-lock module and pumping until a vacuum of $<10^{-7}$ torr is obtained. The load-lock valve is then opened and the sample holder extended into the load-lock where a sample is transferred and clamped onto it. The sample holder is then withdrawn into the growth chamber, the load-lock valve closed, and the growth chamber pumped back down to $<10^{-8}$ torr. During the preliminary bake-out and stabilization of the binary and elemental furnaces, the sample is protected by covering it with a portion of the shutter. Once the CdTe furnace temperature has stabilized, the sample surface is exposed and heated to remove any surface contaminants. Following the thermal etch the CdTe furnace shutter is opened and a CdTe buffer layer grown. To grow HgCdTe, the sample surface is first protected as described previously and the Cd and Te flux rates set using the ionization gauge adjacent to the growth position. The Hg furnace temperature is then raised to the required setting for the run, and the bellows compressed to pipette Hg into the furnace. After the Hg furnace temperature has stabilized, the sample is uncovered and the Hg, Cd and Te_2 shutters opened to commence growth. During the running of the Hg-furnace, the Hg level is monitored and kept constant by the use of a small probe which forms an electrical make-and-break switch with the surface of the Hg. This procedure is believed to result in a more constant flux density by

maintaining a constant flux geometry and by reducing variations in the thermal loading on the furnace. The growth run is terminated by closing the Cd and Te_2 furnace shutters and cooling the sample in the Hg flux to protect the surface. Mercury is removed by expanding the metal bellows of the Hg reservoir so that all of the Hg is withdrawn from the furnaces. The sample surfaces can also be protected by epitaxially depositing a thin layer of CdTe.

For these experiments, four ovens were charged with CdTe, Cd, Te_2 and Hg, respectively. The CdTe was high-purity material obtained from the II-VI Corporation and the elemental source materials were respectively of 6(Cd), 5(Te) and 7(Hg) nines purity and obtained from the United Mineral Chemicals Corporation. All of the solid materials were etched to remove oxide layers before being loaded into the furnace. The CdTe substrates were obtained from the II-VI and Eagle-Picher Companies. Because of the present quality of substrate materials and the difficulty in preparing good surfaces, CdTe buffer layers were grown before the growth of HgCdTe and HgTe . These investigations are described in the next section.

4. MATERIAL ANALYSIS AND PROPERTIES

In order to obtain the best substrate surface conditions for the MBE growth of HgCdTe and to determine the conditions for growing CdTe-HgCdTe heterostructures and CdTe-HgTe superlattice structures, the crystalline properties of epitaxial layers of CdTe on bulk CdTe substrates were first examined. This investigation is especially important because at present the quality of bulk CdTe does not equal the perfection of most III-V substrate materials such as InSb, GaAs and InP. The CdTe substrates used in this work were orientated within 0.5° of the $\langle 111 \rangle$ direction, polished on the A face, and typically had dislocation densities in the $10^5 - 10^4 \text{ cm}^{-2}$ range. Before growth, they were degreased and cleaned by sequential rinses in trichlorethylene, methanol, and D. I. water and then etched for 2 min. in a 1% Br-methanol solution to remove a 25 micron surface layer. After further rinses in methanol and DI water, they were blown dry with dry nitrogen gas and bonded to Mo holders using pure In. The final surface preparation was performed in the growth chamber and consisted of a thermal etch at 350°C for 10 minutes. It is estimated that this procedure removes hydrocarbon contamination on the surface. Simultaneously with the substrate cleaning, the CdTe furnace was baked out and its temperature set to give a growth rate of $2 \text{ } \mu\text{m/h}$. CdTe layers were then grown for a range of deposition temperatures and growth rates. An example of the structures that were grown in order to

investigate the crystalline properties of CdTe is shown in Fig.

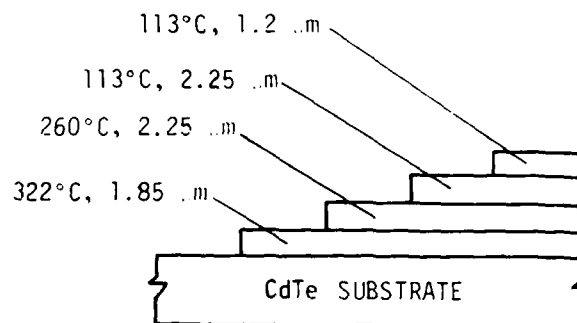


Figure 4. Structure used for material evaluation.

4. For the example shown, the substrate was immediately cooled to approximately 320°C after the thermal etch, partially covered with the shutter, and a 2 micron thick layer of CdTe was grown. The shutter was then indented by a further 2 mm, the substrate cooled to 260°C, and a 2.25 micron thick CdTe layer grown. This procedure was repeated either for progressively lower substrate temperatures and constant CdTe flux rates, as depicted in the figure, or for constant substrate temperatures and different growth rates and times. The layer thicknesses were then measured and their surface quality examined under a microscope. Typically, the surfaces were very smooth and shiny and showed well defined and abrupt steps resulting from the use of the shutter.

The surface properties of each growth step were investigated by reflection electron diffraction (RED), ultra-violet reflectance, and large angle X-ray diffraction. The RED patterns measured on each surface for the structure shown in Fig. 4 are shown in Figs. 5a-5d. The well defined spot pattern observed Fig. 5a is characteristic of a well ordered single crystal surface with a surface roughness of 100°\AA . The circular rings, however, are an indication of the presence of some polycrystalline material. The reflection from the first grown CdTe layer is very weak, but is typical of the pattern observed on an epitaxial surface. For the next layer (Fig. 5b) the RED pattern is better defined and exhibits strong streaking as a result of the emergence of planar growth. The clarity and intensity of this pattern continues to improve with each growth step as depicted in Figs. 5c and 5d. It should be noted that this improvement in crystal quality occurs as the substrate growth temperature is lowered. Similar improvements in the quality of the epitaxial CdTe layers were observed for a variety of structures grown by this method. An excellent RED pattern was also observed from a 2 micron thick CdTe layer grown at room temperature on a stepped structure consisting of 2 micron thick CdTe layers grown at temperatures of 330, 265, and 103°C , respectively. Following the RED evaluation, the use of u.v. reflectance to measure the quality of CdTe layers was investigated. The u.v. spectra of CdTe has well defined peaks at 234, 320, and 276 nm which are associated with the X-state, and

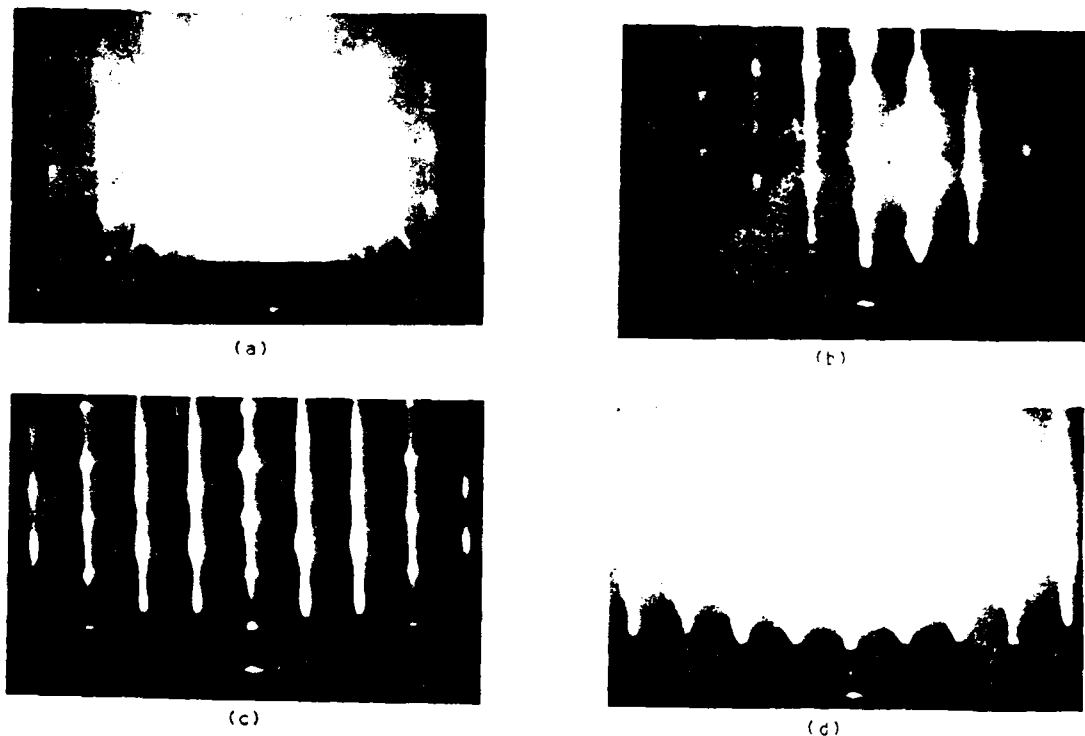


Figure 5. Reflection electron diffraction patterns obtained from sample shown in Figure 4. ((a) substrate, (b), (c), and (d) are the second, third and last deposited layers, respectively)

spin-split L-state positions, respectively, in the Brillouin zone.¹⁰ These features are a consequence of the long-range order in the crystal, and thus their strength and definition are a measure of the crystalline perfection of the surface. Because the peaks are associated with strong optical absorption, the penetration depth of the u.v. radiation is very shallow, between 1-10 nm. Myers et al.¹⁰ have attributed additional structure at 354 and 310 nm in thin CdTe layers to the formation of stacking

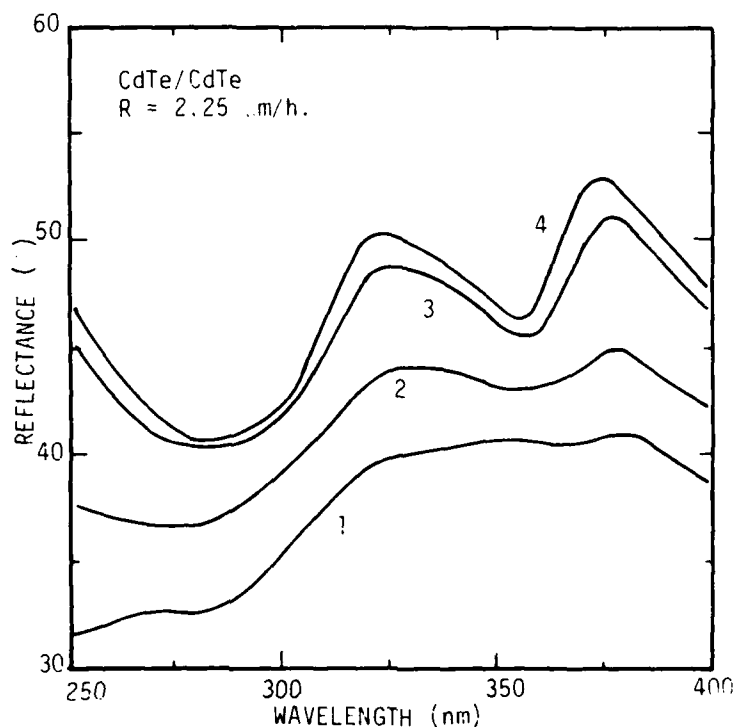


Figure 6. Ultra-violet reflectivity of MBE grown CdTe on (111) orientated CdTe substrate.

faults associated with a wurzite phase of CdTe. Thus, measurement of the u.v. reflectance spectrum should give significant information on the crystalline perfection of epitaxial layers and because of its shallow penetration depth how it changes during growth.

The spectra taken for the sample depicted in Fig. 4 are shown in Figure 6. For the first grown layer the spectra between 300-400 nm is not well defined but shows the presence of two

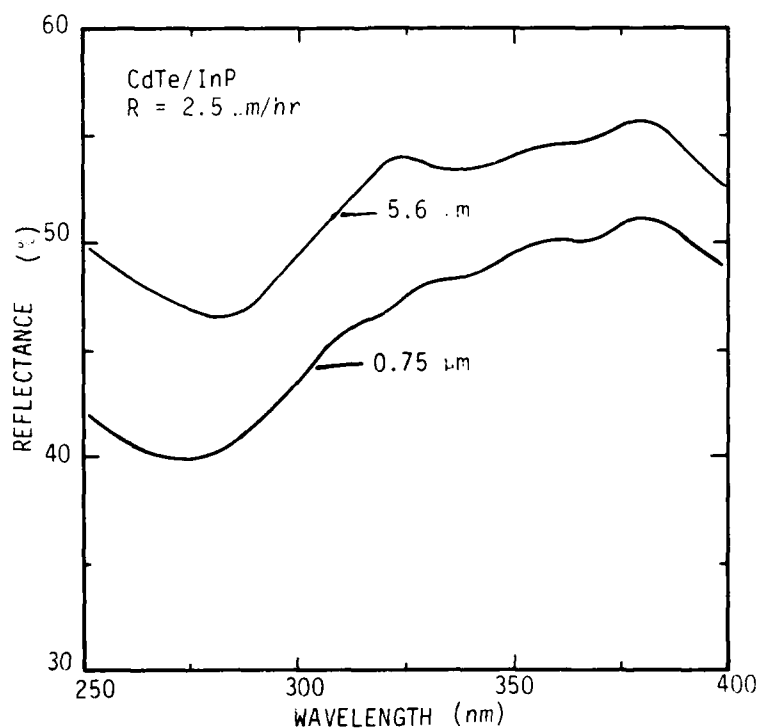


Figure 7. Ultra-violet reflectivity of CdTe grown on (100) orientated InP substrate.

broad peaks centered at 320 and 280 nm and two minor features at 270 and 250 nm. With each additional epitaxial growth, the strength and definition of the peaks at 320 and 374 nm increases whereas the other features are no longer observed after the growth of 4 microns of CdTe. Spectra 4, which is taken on the last grown surface (at 113°C), is identical with the spectra measured on a damage free CdTe substrate. The u.v. spectra therefore indicate the presence of some stacking faults or

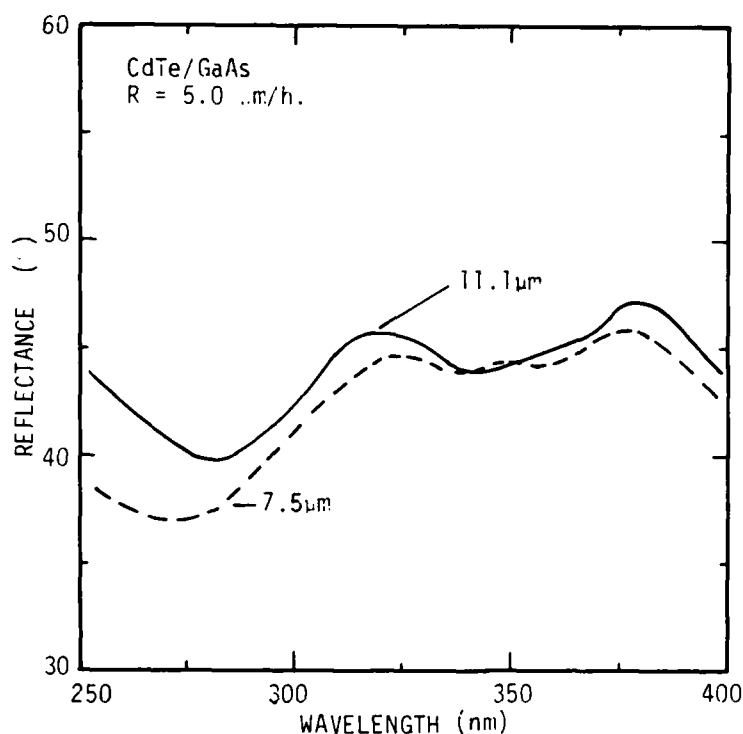


Figure 8. Ultra-violet reflectivity of CdTe grown on (100) orientated GaAs substrate.

wurzite phase at the beginning of the epitaxial growth, but show at that this damage is grown out after approximately 5-6 microns. Thus, it appears that any defects or surface contaminants can be corrected by depositing a thick layer.

The strong tendency for CdTe to recover its crystalline properties has also been observed in depositions on other substrate materials. During the initial characterization runs on

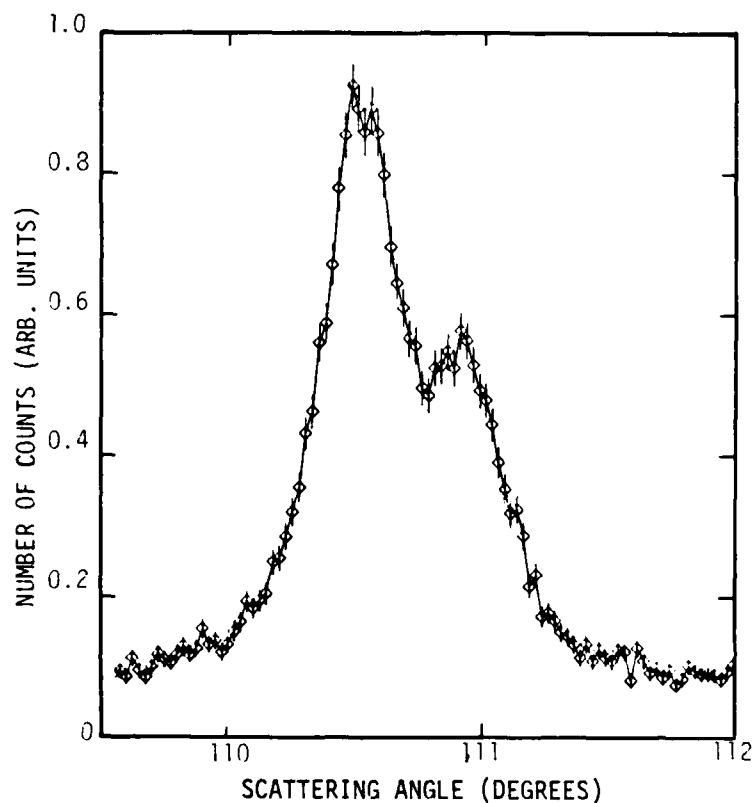


Figure 9. X-ray diffraction spectra of MBE grown CdTe on (100) orientated GaAs substrate.

the system, CdTe was deposited on (100) orientated GaAs and InP substrates. Despite the large lattice mismatch between CdTe and these materials, the optical quality of the the deposited CdTe showed very good surface morphology. Their u.v. and X-ray properties were therefore investigated. Figure 7 shows the u.v. reflectance for a stepped CdTe structure grown on InP for layer thickness up to 5 microns. The data show peaks at 270, 320, 350

and 380 nm indicating the presence of mixed wurzite and zincblends phases. However, as shown for thicker layers, the u.v. spectra becomes sharper indicating a predominately zincblend crystal phase. This evidence is confirmed by large angle X-ray diffraction data. The ability of CdTe to recover its crystalline properties was also observed in depositions on GaAs. These growths were performed during the initial characterizations of

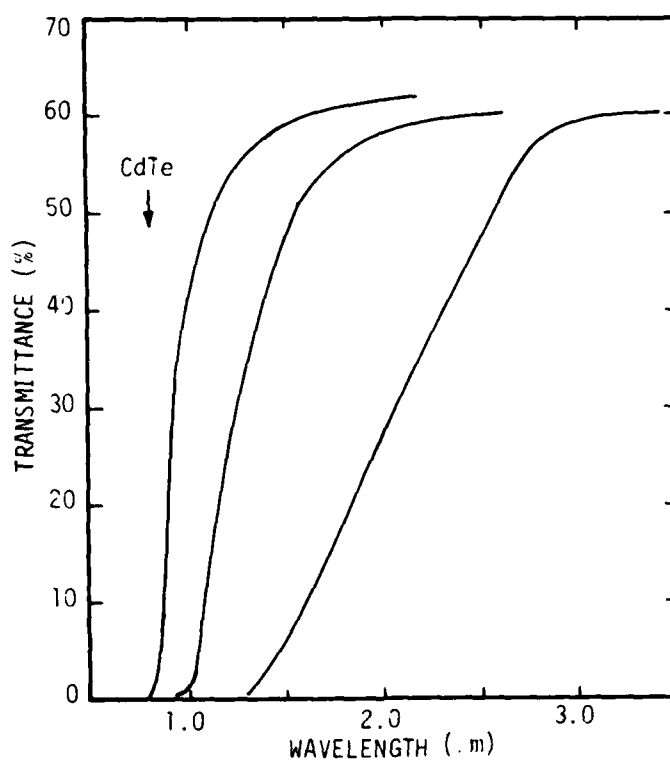


Figure 10. Infrared transmittance spectra of MBE grown $\text{Hg}_{1-x}\text{Cd}_x\text{Te}$ layers.

the system and optical investigations showed that the quality of the CdTe was reasonable despite the large lattice mismatch between the two materials. Figure 8 shows the u.v. reflectivity for a stepped structure with 3.6 and 7.5 μm thick CdTe layer grown on (100) orientated GaAs. As shown, the quality of the spectra increases with growth time and indicates the emergence of a zincblend crystal phase. Examination of the (444) reflection from this sample using copper k_{α} radiation shows that the intensity of the beam increases and its half-width decreases as the CdTe layer thickness increases. For an 11 micron thick CdTe layer grown on GaAs, the (444) reflection is sufficiently narrow as shown by Figure 9 for the $k_{\alpha 1}$ and $k_{\alpha 2}$ lines of the copper target to be resolved and show that the half-width of the scattered X-ray beam is approximately 0.25° . These results were obtained for a deposition temperature of 260°C . Thus, it is possible that performing the initial depositions at higher temperatures, followed by a reduction in the substrate temperature, will result in improved crystal quality as found for CdTe and recently reported by Cheung.¹¹

Following these initial growth runs and characterizations, HgCdTe layers were grown on epitaxially grown CdTe buffer layers. These growths were performed for substrate temperatures between 180 - 200°C and constant Te_2 and Hg flux rates. The Te_2 flux rate was the same as used to grow CdTe, and the Cd flux was reduced in small increments from the level required to grow stoichiometric CdTe. The Hg flux rate was kept constant and was

approximately two orders of magnitude larger than either the Te_2 or Cd flux rates. The crystallographic properties and thickness of these layers were very similar to the CdTe layers. The transmission data taken on three high x-value samples are shown in Figure 10. The transmission cut-on of the layers is observed to move to longer wavelengths from 0.8 to 2 microns as the Cd flux density is decreased, showing that the Hg composition in the layer is increasing. For these alloys an absorption coefficient of 500 cm^{-1} is expected at the energy bandgap. This corresponds to a transmission of 30% for a 3 micron layer. Thus, the energy bandgaps are calculated to occur at 1.38, 0.81, and 0.58 eV, corresponding to alloy compositions with x-values 0.9, 0.85 and 0.5, respectively.

Because the magnitude of the absorption coefficient, α , for interband transitions decreases with alloy composition, it is very difficult to obtain an accurate determination of the bandgap energy from infrared transmission measurements on thin films of low alloy composition. For these samples the absorption coefficient spectra were calculated. An example of the data obtained from samples grown with flux rates estimated to produce x-values of 0.2 and 0.3 is shown in Fig. 11. Also shown in the figure is a calculation of the low-temperature absorption coefficient spectrum for a HgCdTe alloy with a bandgap energy corresponding to 10 microns. This calculation was performed for the full Kane energy band structure using the accepted band parameters for the HgCdTe alloy system. The calculated and

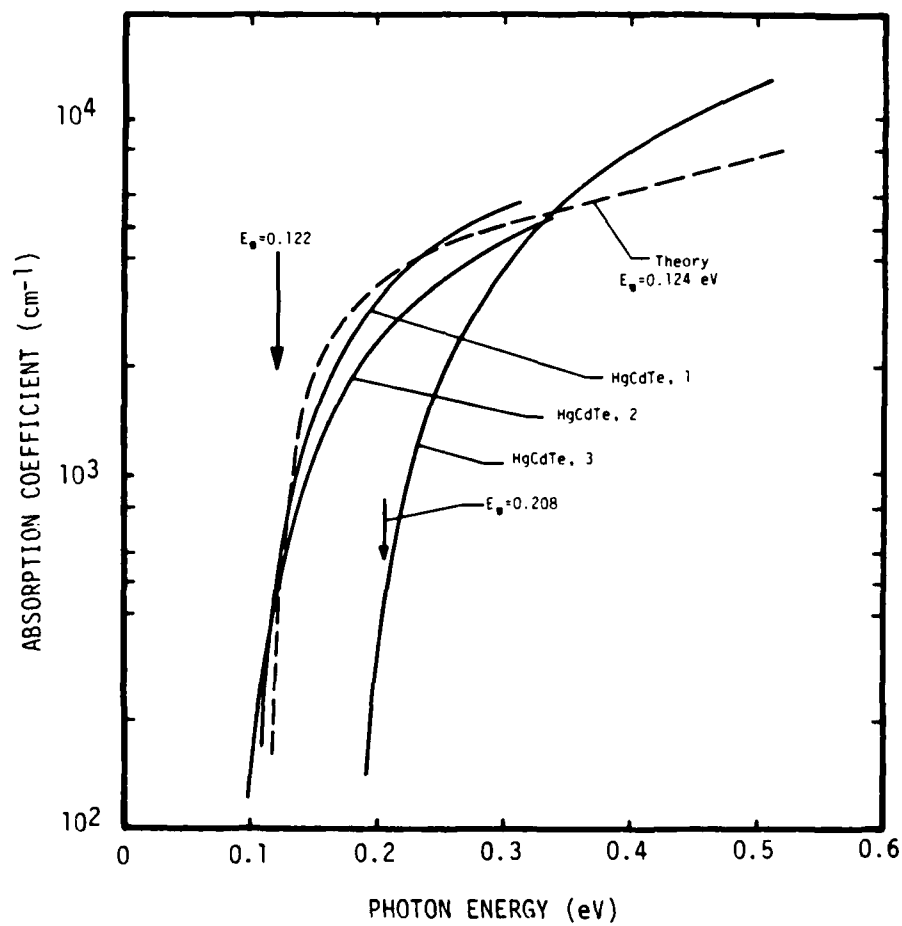


Figure 11. Absorption coefficient spectrum for low x-valued MBE grown $\text{Hg}_{1-x}\text{Cd}_x\text{Te}$ layers.

experimental curves are observed to have similar spectral dependencies. At high energies the absorption coefficients decrease uniformly with decreasing photon energy and fall abruptly near the energy gap. The difference between the magnitude of the experimental and theoretical curves is less than 50% and falls within the experimental errors and theoretical accuracy in predicting the absorption coefficient spectrum for these alloys. By assuming that the absorption coefficient is 200 cm^{-1} at the bandgap energy, the energy gap for these samples is found to occur at 0.12 and 0.21 eV, respectively, corresponding to x-values of 0.17 and 0.23 if Schmit and Stelzer's determination of the dependence of bandgap energy on alloy composition and temperature is used.¹² Although at present these values are not very close to the targeted compositional values, the spectra measured for samples 1 and 2 demonstrate the reproducibility that can be obtained from run to run. The experimental curves are observed to be only slightly broader than the theoretical curve. Because this can easily be accounted for by thermal broadening, we believe that the layers are very uniform along the growth direction. Measurements of the transmission cut-on wavelength performed at different locations on the samples surface suggest that the compositional uniformity is better than 1% over a 1 cm^{-2} area.

5. CONCLUSIONS

A MBE system specifically designed for the growth of HgCdTe alloys has been constructed and used to grow CdTe and $\text{Hg}_{1-x}\text{Cd}_x\text{Te}$ layers with $0.9 > x > 0.17$. X-ray diffraction measurements show that at present the quality of CdTe substrates and/or surface preparation procedures cause an initial degradation of the quality of the layer, but that these defects can be grown out. For CdTe layers thicker than 5 microns, good quality surfaces are obtained. Epitaxial deposited CdTe has been shown to be remarkably adaptable and (111) orientated CdTe layers have been grown on (100) orientated GaAs and InP substrates. Preliminary growth runs have produced good quality $\text{Hg}_{1-x}\text{Cd}_x\text{Te}$ layers with spectral response characteristics extending out to 10 microns at 300K.

Finally, we note that although the growth of CdTe and HgCdTe by MBE is very new, the progress obtained in this and other investigations¹³⁻¹⁵ is sufficiently encouraging to suggest that it will have long range application for the growth of complex device structures for infrared detection and generation. These results suggest that MBE will make it possible to grow: n^+-n-p high-speed homopolar photodiodes; a wide range of CdTe - $\text{Hg}_{1-x}\text{Cd}_x\text{Te}$ and $\text{Hg}_{1-x}\text{Cd}_x\text{Te}-\text{Hg}_{1-y}\text{Cd}_y\text{Te}$ heterostructures; and a variety of superlattice structures. MBE can also be used to passivate, separate, and connect device structures by the use of insitu masking as well as by the epitaxial growth of high resistivity or

doped CdTe layers. These capabilities could make it possible to develop integrated focal plane array structures in a sequential growth process, thus requiring very little subsequent processing.

This potential obviously demands further studies of this growth technique.

6. TECHNICAL PRESENTATIONS AND PUBLICATIONS

During the period of this contract the following presentations and publications were generated.

Presentations

1. "Molecular beam epitaxial growth and characterization of $\text{Hg}_{1-x}\text{Cd}_x\text{Te}$ ", SPIE Conference on the Technical Issues in Infrared Detectors and Arrays, Arlington, VA, April, 1983. (Invited)
2. "Molecular beam epitaxial growth of the $\text{Hg}_{1-x}\text{Cd}_x\text{Te}$ system", Third Annual Symposium of the Tennessee Valley Chapter of the American Vacuum Society, Knoxville, TN, May, 1983. (Invited).
3. "Molecular beam epitaxial growth of CdTe, HgTe and $\text{Hg}_{1-x}\text{Cd}_x\text{Te}$ alloys," 1983 Meeting of the IRIS Specialty Group on Infrared Detectors, August 1983, Boulder, Co.
4. "Molecular beam epitaxial growth of CdTe, HgTe and $\text{Hg}_{1-x}\text{Cd}_x\text{Te}$ Alloys", MBE Workshop, Atlanta, Ga. October, 1983.

Publications

1. C. J. Summers, E. L. Meeks and N. W. Cox, "Molecular beam epitaxial growth and characterization of $\text{Hg}_{1-x}\text{Cd}_x\text{Te}$," Proceedings of SPIE 409, 1-8, (1983).
2. C. J. Summers, E. L. Meeks and N. W. Cox, "Molecular beam epitaxial growth of CdTe, HgTe and $\text{Hg}_{1-x}\text{Cd}_x\text{Te}$ alloys", to be published in the 1983 Proceedings of the IRIS Specialty

Group on Infrared Detectors, and in the Journal of Vacuum
Science and Technology, 1984

7. TECHNICAL PERSONNEL

The technical personnel which contributed to this program were;

Dr. C. J. Summers

Dr. E. L. Meeks

Dr. N. W. Cox

all of these investigators are with the Engineering Experiment Station, Georgia Institute of Technology, Atlanta, Georgia 30332.

8. REFERENCES

1. M. B. Reine, A. K. Sood and T. J. Tredwell, "Photovoltaic Infrared Detectors" Semiconductors and Semimetals Vol. 18, (R. K. Willardson and A. C. Beer, Eds., Academic Press, New York, N. Y. 1981). p. 201.
2. "Assessment of Mercury Cadmium Telluride Materials Development," NMAB Publication 377, National Academy of Sciences, Washington, D.C. 20418.
3. M. S. Lamir and K. J. Riley, "Performance of PV HgCdTe Arrays for 1-14 μ m Applications," IEEE Trans. Electron Devices ED-29, 274-279 (1982).
4. The 1981 and 1983 U.S. Workshops on the Physics and Chemistry of Mercury Cadmium Telluride, J. Vac. Sci. Technol. Vol. 21 No. 1 (1982). J. Vac. Sci. Technol. A, Vol. 1, No. 3, 1983).
5. A. Y. Cho and J. R. Arthur, Progress in Solid State Chemistry 10, 157 (1975).
6. R. F. C. Farrow, G. R. Jones, G. N. Williams, P. W. Sullivan, W. J. O. Boule and J. T. Wotherspoon, "The Vaporization of $\text{Hg}_{1-x}\text{Cd}_x\text{Te}$ Crystals - a Case of Gross Incongruency," J. Phys. D.: Appl. Phys. Vol. 12, L117-L121, (1979).
7. R. E. Honig and D. A. Kramer, "Vapor Pressure Data for the Solid and Liquid Elements," RCA Review, pp. 285-305. (1969).
8. D. L. Smith and V. Y. Pickhardt, "Molecular Beam Epitaxy of II-VI Compounds", J. Appl. Phys. 46, 2366-2374, (1975).
9. H. Holloway, D. K. Honke and E. M. Logothetis, "Epitaxial Growth of Small Bandgap Semiconductors," J. Vac. Sci. Technol., 8, 146 (1971).
10. T. H. Myers, S. W. Edwards and J. F. Schetzina, "Optical Properties of Polycrystalline CdTe Films," J. Appl. Phys., Vol. 52, pp. 4231-4237, 1981.
11. J. T. Cheung and T. Magee "Recent Progress of LADA Growth of HgCdTe and CdTe Epitaxial Layers," J. Vac. Sci. Technol. A, 1, 1604-1607 (1983).
12. J. L. Schmit and E. L. Steizer, "Temperature and Alloy Compositional Dependences of the Energy Gap of $\text{Hg}_{1-x}\text{Cd}_x\text{Te}$," J. Appl. Phys. 40, 4865 (1969).

13. J. P. Faurie and A. Million, "Molecular Beam Epitaxy of II-VI Compounds: $\text{Cd}_x\text{Hg}_{1-x}\text{Te}$ ", J. Cryst. Growth, Vol. 54, pp. 582-585, (1981).
14. J. P. Faurie and A. Million, " $\text{Cd}_x\text{Hg}_{1-x}\text{Te}$ n-Type Layers Grown by Molecular Beam Epitaxy", Apply. Phys. Lett., Vol. 41, 264-266, (1982).
15. T. H. Myers, Lo Yawcheng, J. F. Schetzina and S. R. Jost, "Properties of CdTe/InSb Heterostructure Prepared by Molecular Beam Epitaxy," J. Appl. Phys. 53, 9232-9234 (1982).

END

DATE
FILMED

7 - 84

DTIC